Deformation Bands, the LEDS Theory, and Their Importance in Texture Development: Part I. Previous Evidence and New Observations

D. KUHLMANN-WILSDORF, S.S. KULKARNI, J.T. MOORE, and E.A. STARKE, JR.

The present state of knowledge regarding "regular" deformation bands (DBs) is reviewed in the light of some recent observations on DBs in compressed polycrystalline aluminum. These are slablike volume elements within which different selections of slip systems operate, always fewer than required for homologous deformation, in opposition to the assumption that grains deform as units which are common to all, the Sachs, the Boas and Schmid, and the Taylor/ Bishop and Hill models. The need for a better integration of this knowledge with not only the origin of deformation textures but also more generally with the theory of plastic deformation is pointed out.

I. INTRODUCTION—PRIOR EVIDENCE ON DEFORMATION BANDS

A. *The Four Most Important Models of Polycrystal Deformation*

THE geometry and mechanics of single crystal deformation in terms of glide on close-packed lattice planes in close-packed lattice directions, with the different possible slip systems selected in accordance with the highest resolved shear stress, was well established even before dislocations were discovered, as documented in the foundational book by Schmid and Boas.[1] We now know, of course, that the carriers of this kind of deformation are glide dislocations. We also know that in glide they respond virtually instantaneously to resolved shear stresses above the level of the "friction stress," τ_0, but respond very sluggishly, if at all, to normal stresses, namely, *via* climb, which is negligible below about one-half of the absolute melting temperature, $T_M/2$.

Initially, it seemed to be an easy matter to account for polycrystalline deformation as the collective effect of the individual grains, each behaving much like a single crystal under the same imposed stress, as done in the Sachs model of texture formation.[2] Correspondingly, from the outset, most of the relevant experimental and theoretical work was devoted to the simplest case, *i.e.*, axisymmetric flow under uniaxial stress such as is approximated in tensile testing, small-strain compression, wire drawing, or extrusion. However, single- or double-glide deformation, as expected under tensile stress, cannot account for the shape changes that are obviously necessary to maintain cohesion among the grains. Besides, attainment of the same critical resolved shear stress on the most highly stressed slip system(s) would require different tensile stresses from grain to grain. Hence, the Sachs model implies both strain and stress incompatibility at grain boundaries.

Chronologically, the next important model was due to Boas and Schmid,[3] who proposed that always the three most highly stressed slip systems act simultaneously and produce that lattice orientation in the grains which is stable under such triple slip. The stable orientations would correspond to the ⟨112⟩ axis orientation produced by ⟨110⟩ {111} double-glide in cubic crystals under tension. Yet, this model still does not solve the stress incompatibility nor the coherency problem at grain boundaries, the latter since von Mises[4] had already shown arbitrary shape changes to require five independent slip systems. Accordingly, Taylor[5] postulated that all grains deform homologously (the Taylor model) and, like his predecessors, assumed that each grain deforms as a unit.

Taylor further proposed that the necessary five slip systems be selected so as to accommodate the imposed shape change with a minimum of slip summed over all activated slip systems. This is the "Taylor criterion" or "minimum strain criterion," or (somewhat confusingly) also the "minimum work criterion," since at a given flow stress, minimum strain is equivalent to minimum internal plastic work. Albeit, in performing the numerical calculations for axisymmetric flow as a function of lattice orientation in the stereographic standard triangle for fcc lattices with ⟨110⟩{111} slip, Taylor found that the kind of symmetry required for five simultaneously acting slip systems in fact yielded six or eight equally favored systems from which to choose. He thus could not make a unique selection of the slip systems and, as a consequence, for many orientations found two possible incremental lattice reorientations that could be combined to render any intermediate reorientation. Worse, the internal stresses implied in the Taylor model, differing from the imposed stress, still produce stress incompatibility at the grain boundaries. On the positive side, Taylor's computations predict that in tension all orientations near ⟨100⟩ move toward ⟨100⟩ and those near ⟨111⟩ toward ⟨111⟩, in agreement with the widely observed "double fiber texture" generated though extensive uniaxial deformation to be further discussed subsequently.

Bishop and Hill[6] extended the Taylor model to arbitrary

D. KUHLMANN- WILSDORF, University Professor of Applied Science, Department of Physics, J.T. MOORE, Research Scientist, Department of Materials Science and Engineering, and E.A. STARKE, Jr., University Professor of Materials Science and Oglesby Professor of Materials Science and Engineering, Department of Materials Science and Engineering, are with the University of Virginia, Charlottesville, VA 22903. S.S. KULKARNI, formerly Graduate Student with the Department of Materials Science and Engineering, University of Virginia, is Research Scientist, Advanced Materials Division, Materials Research Corporation, Orangeburg, NY 10962.

Manuscript submitted July 6, 1998.

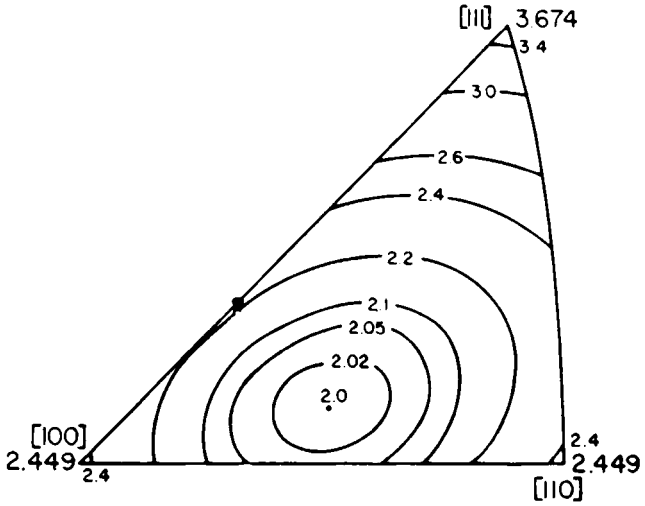

Fig. 1—Taylor factors, *M*, for tensile testing of fcc single crystals, appropriate also to the Sachs model[2] for fcc polycrystalline specimens under tension.

imposed strains and proposed that the active slip systems are those that have the highest resolved shear stress (the so-called "maximum work criterion"). For fcc, they also found the same six or eight simultaneous slip systems rather than five, as Taylor also had, and noted that Taylor's minimum strain (minimum internal work) and their maximum (external) work criteria are the same at least for uniaxial strain. Chin and Mammel[7] went on to show that the Taylor[5] and Bishop and Hill[6] theories are entirely equivalent. While the proof is complex, the indicated equivalence basically arises because, say in tensile straining, the Taylor factor, M (the reciprocal of the Schmid factor, m), relates shear strain, γ, to tensile strain, ε, in the inverse way as resolved shear stress, τ, to tensile stress, σ, namely, as

$$\gamma = M\varepsilon = \varepsilon/m \text{ and } \tau = \sigma/M = m\sigma \qquad [1]$$

Now, in both methods, the selected five (from the possible six or eight depending on orientation) slip systems turn out to have the same resolved shear stress, *i.e.*, the same M values. Therefore, in the Taylor model, minimizing the sum of the shear strains maximizes the sum of the applied stresses and thereby the external work input, *i.e.*, under the constraint that only the most highly stressed slip systems operate, as in the Bishop and Hill model. Either way, the internal and external virtual work are the same, as they must be, namely, $\sigma\, d\varepsilon = \tau\, d\gamma$.

B. *Effect of Taylor Factors and Avoidance of Intersecting Glide*

It is highly instructive to compare the Taylor factors that are predicted for axisymmetric flow by the three different models, as in Figures [1] through [3], relevant to the Sachs,[2] Boas and Schmid,[3] and Taylor[5]/Bishop and Hill[6] models, respectively, the last of these according to the computations of Chin and Mammel.[8] As seen, with increasing number of simultaneously acting slip systems, the Taylor factors rise. Namely, in order to achieve a rising number of equally stressed slip systems, the most highly stressed must be increasingly rotated away from their favorable orientations and thereby their Taylor factors be increased so as to let the Taylor factors of the initially less favorable systems rise. Therefore, simply as a matter of geometry, it requires a higher applied stress to simultaneously activate a larger number of slip systems.

In addition to this geometrical effect, there exists a physical, and generally still more powerful, reason why the flow stress rises with the number of simultaneously active systems. This is the difficulty of intersecting active slip systems. This has been known for some time, first through "overshooting" in α-brass type alloys (the so-called "planar-glide materials") that was observed in the twenties.[9,10] Second, for "wavy-glide materials" (comprising the great majority of pure cubic metals under common straining conditions), metallographically the impediment against intersecting slip is intuitively obvious from the visual appearance that slip band intersections tend to be avoided, albeit by no means completely. Third, as was established with good confidence by means of electron microscopy, at slip band intersections from moment to moment, one or the other of the bands may be active but apparently never both simultaneously.[11] Fourth, inactive slip systems work harden more rapidly than active ones, as so dramatically manifested in overshooting. This is the phenomenon of "latent hardening" that is also present in wavy-glide, without overshooting. It typically amounts to about 40 pct excess flow stress for intersecting slip systems but is (nearly) absent for coplanar glide, *e.g.*, Jackson and Basinski[12] and Wu *et al.*[13]

Clearly, then, avoidance of local polyslip (a) is a pervasive characteristic of dislocation-based plasticity and (b) causes an increase of flow stress with increasing number of simultaneously acting slip systems. It stands to reason, therefore, that grains will not deform homologously but instead will break up into regions of one or two, here and there, perhaps three, simultaneously acting slip systems. Thereby, the total elastic strain energy is decreased as the flow stress is lowered through a decreased number of active slip systems but at the expense of a lesser increase of the elastic energy of local internal incompatibility stresses. As recently shown by Becker[14] and Dawson and co-workers[15,16] finite element modeling of sufficiently small mesh size does indeed predict grain fragmentation during deformation of polycrystals. A few years ago, corresponding evidence was discovered in dislocation microstructures.[17] This was pursued and refined in terms of dislocation theory[18,19] without realizing the connection to, indeed overlooking the existence of, "regular" deformation bands[20] (DBs), the principal topic of the present article.

Regular DBs (as distinct from other forms of band-like effects due to glide[20]) are slab-shaped volume elements within which the number of active slip systems is too small for homologous deformation and which are arranged such that pairs or groups of contiguous bands together (nearly) fulfill the Taylor criterion. On account of the different slip systems operating in them, families of deformation bands have an overall unitary orientation, and the boundaries between bands are true geometrically necessary boundaries (GNBs). DBs are thus analogous to the "cell blocks" of References 17 through 19. However, first, cell blocks are normally not slablike and, second, in TEM, it is impossible

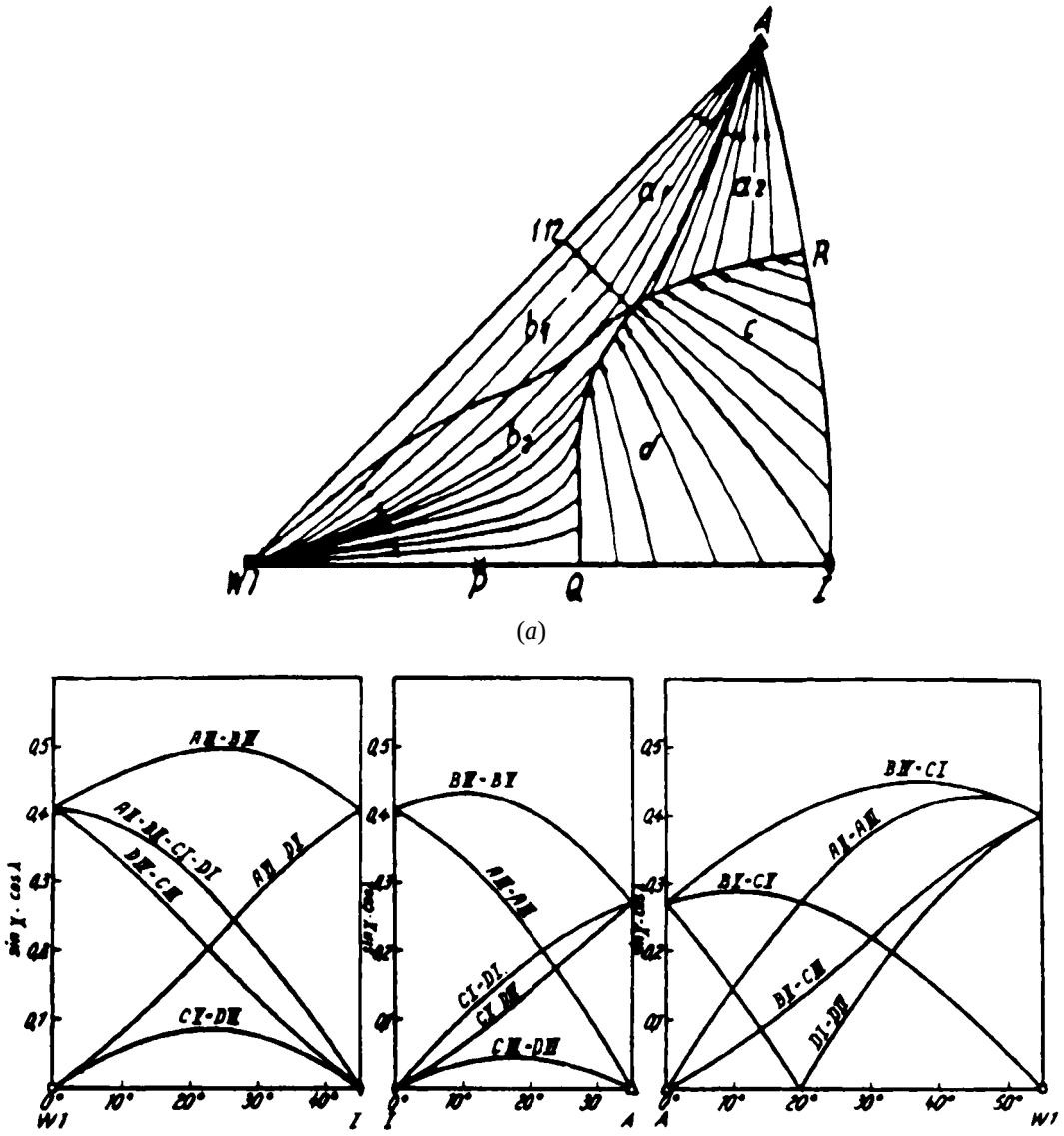

Fig. 2—(*a*) Distribution of areas with the same three most highly stressed slip systems of slip planes (letters) and slip directions (Roman numerals) in fcc crystals under tension. Using Schmid and Boas's[1] nomenclature, B IV is the most highly stressed slip system throughout. The second and third systems are, in order, a_1: C I and B V; a_2: B V and C I; b_1: C I and A III; b_2: A III and C I; c: B V and A III; and d: A III and B V (Fig. 3 of Boas and Schmid[3]). (*b*) Schmid factors, $m = 1/M$, along the periphery of the standard triangle above, namely, between [100] (symbol W1) and [110] (symbol I) *at left*, between [110] and [111] (symbol A) *in the middle*, and between [111] and [100] *at right*. Except at [100] and [111], the averaged Taylor factors are moderately higher than for the same orientations in Fig. 1 (Fig. 2 from Boas and Schmid[3]).

to reliably distinguish GNB due to different slip system selections on either side,[21] and from "incidental boundaries" (IBs), meaning cell wall boundaries that arise through mutual trapping of glide dislocations.[21] Specifically, in wavy-glide, because of ordinary work hardening, the DBs, like cell blocks, are subdivided by the "mosaic block structure," *i.e.*, by the IBs of mutually misoriented dislocation cells. It only gradually became clear that many previously presumed GNBs are in fact mature cell walls.[22,23,24] To add to the complexity of the structures, note that throughout their evolution from nucleation[23] until becoming grain boundaries, cell walls have a dual IB/GNB nature (Section 18 of Reference 25), although they are initially by far best understood as IBs. In this connection, note that Duly *et al.*[26] have in their study of deformation in Al-1 wt. pct Mg correlated the deformation structure observed by TEM with the deformation bands observed under optical microscopy.

Based on the preceding facts in terms of deformation texturing, the different texture components are clearly the lattice orientations in the DBs, while the dislocation cell structure in the DBs of wavy-glide materials causes the "fuzziness" of deformation textures, which persists, and even continues to increase, to the highest strains. And further, it is evidently not necessary that volume elements deforming by a specific, or any particular selection of, active slip system(s) have slablike shape or be arranged in some recognizably regular pattern. Therefore, in agreement with References 14 through 16, many cell blocks (CBs) seen in TEM will indeed have slip system selections distinct from their neighbors and thus be surrounded by true GNBs (*e.g.*,

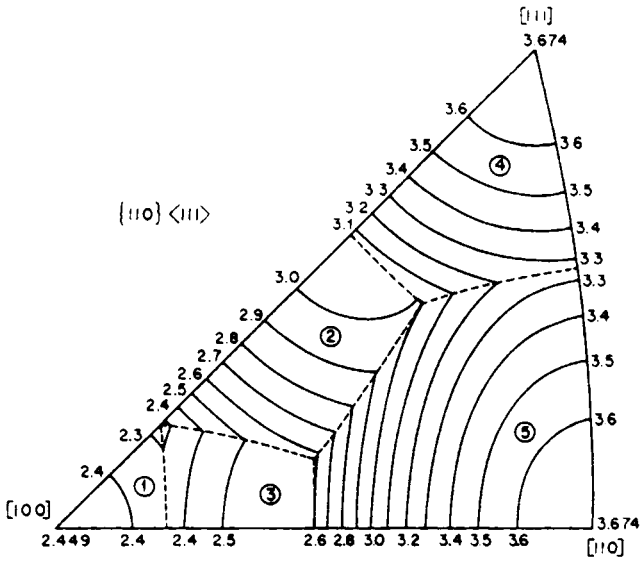

Fig. 3—The Taylor factors for the five most highly stressed slip systems required in the Taylor[5] and Bishop and Hill[6] models for homologous deformation in a tensile-tested fcc polycrystal according to Chin and Mammel[7] (Fig. 2 from Chin and Mammel[7]).

Fig. 4—Deformation bands in a transverse section of polycrystalline iron wire reduced 30 pct by drawing. Dilute nitric etch. Magnification 100 times (Fig. 3 from Barrett and Levenson[28]).

as in Reference 47). However, as will be further discussed in Section D, *via* TEM alone, these can hardly be distinguished from the presumably great majority of CBs that are not of this kind.

C. *Evidence on Occurrence and Properties of Deformation Bands*

The reason for the initial failure of making the connection between GNBs and DB boundaries was the, even now still pervasive, relative obscurity of the phenomenon of regular deformation banding. This difficulty persists for two reasons. (a) Since it is often assumed that optical microscopy is a poorer means of investigation than electron microscopy, optical microscopy is frequently not performed. Even when it is performed, deformation banding often goes un-noticed, as it is not easily revealed through etching. (b) In spite of its very evident impact on texture modeling, through the decades, deformation banding has been largely ignored in favor of the Taylor/Bishop and Hill assumption (shared by the Sachs and Boas/Schmid models) of homologous deformation of whole grains. This widespread neglect is most surprising because the nature and important role of DBs in plastic deformation and texture formation have again and again been clearly recognized by eminent researchers. Foremost among them is Barrett and co-workers[27–32] who, partly with Levenson, performed extensive studies on DBs in iron after compression[27] (up to 97 pct compressed) and after drawing, swaging, and elongation in tension,[28] as well as in compressed aluminum,[29] and with Steadman made similar investigations on rolled copper.[30] An optical micrograph, taken from Reference 28 and showing deformation bands in polycrystalline iron, is given in Figure 4.

Barrett summarized his findings in his book.[31, 32] He had set out to test the predictions of the Boas and Schmid[3] and of the Taylor model[5] and found them wanting. Indeed, persistent discrepancies between the observed and theoretically expected deformation textures have been the rule rather than the exception. In response, numerous modifications and refinements have been proposed. In the framework of homologous deformation, a principal subject of consideration here has been possible rules for the selection of the five necessary from the possible six or eight in fcc metals. Another important approach has used the "relaxed constraint" concept. This approach permits deviations from homologous deformation, *e.g.*, in the short directions of grains that may have become pancake shaped or filamentary through rolling or drawing, respectively. The DB evolution may be accepted as a rather extreme form of relaxed constraints, but in the traditional models, by and large, the concept that grains deform as units has been retained. In a survey on rolled fcc metals, Hirsch *et al.*[33,34] considered DBs (and twinning that is not dealt with in the present article) but still assumed that grains retain different unitary orientations and concluded that DBs "have no significant influence on texture formation." However, more recently, effects of inhomogeneous deformation of grains have been increasingly, and with increasing success, incorporated into texture modeling. Albeit there is still much debate over the lack of quantitative agreement between the modeled textures and those seen experimentally, as indicated in the many examples cited in papers of the ICOTOM series of conferences[35,36] and a recent book on the subject.[37]

Focusing, then, on the experimental evidence on DBs, already in his early articles, Barrett pointed out that grains commonly split into DBs within which the number and/or selection of simultaneously acting slip systems differed from band to matrix or neighbor band. Barrett also knew that this number always fell short of requirements for homologous deformation and that secondary bands could form in primary bands. Further, in his review of early relevant work, Barrett pointed to the all-but-forgotten yet scientifically outstanding articles by Pfeil.[38,39] From his 1926/7 observations on carefully, uniaxially compressed iron single crystals, Pfeil had already discovered that slip took place on different slip systems within well-delineated bandings. In this connection,

Fig. 5—Etched transverse cross section of an aluminum rod extruded 90 pct at 77 K from a ⟨111⟩ single crystal revealing DBs in polarized light. Magnification 45 times (Fig. 7 from Reed and McHargue[47]).

Barrett expressed surprise that Taylor and Elam[40] missed noticing the deformation bands in iron; even more surprising since their experiments were made on iron single crystals provided by Pfeil (acknowledgment in Reference 40).

Other excellent early studies of deformation bands have been made by Ahlborn[41–44] on wire-drawn (up to 99 pct reduction of cross section) oriented single crystals of fcc metals, including silver and gold[43] and copper, aluminum, and 15 pct-α-brass.[42] For most of these, Ahlborn documented clear patterns of DBs that reflected the crystal symmetry, except that only traces of DBs were found in aluminum. Importantly Ahlborn showed that the already mentioned characteristic ⟨100⟩ − ⟨111⟩ double fiber texture of drawing, on account of which he made his studies, was due to different families of DBs. A quantitative interpretation of Ahlborn's data[44] was achieved by Chin and Wonsiewicz[45] based on DBs. Their analysis abandoned the Taylor model of homologous deformation but retained Taylor's minimum work criterion. Contrary to initial impression, this combination of assumptions is not entirely automatic since, as first pointed out by Chin,[46] DBs can theoretically arise not only through too few slip systems, but also through variations in the selections of any five among the six to eight possible slip systems. However, this case seems never to have been observed.

Perhaps even more remarkable are the studies by Reed and McHargue[47] on extruded ⟨100⟩,⟨110⟩, and ⟨111⟩ oriented aluminum single crystals, again aimed at clarifying the origin of the ⟨111⟩ ⟨100⟩ fiber texture. An example of the DBs they observed in a ⟨111⟩ single crystal extruded 90 pct at 77 K is shown in Figure 5. For the three single crystal orientations chosen by them, their observed DB patterns exhibited the expected fourfold, twofold, and threefold symmetries. But additionally, the DB patterns exhibited a more detailed and overall regular morphology and relative positioning of the ⟨100⟩ and ⟨111⟩ fiber texture components than one would have expected. The patterns depended somewhat on the extrusion temperatures of either 77 K or room temperature, with a higher fraction of ⟨100⟩ component at the lower temperature. In this case, some TEM micrographs were taken in conjunction with the surface imaging. These revealed the ⟨100⟩ component to be represented by roundish, comparatively larger dislocation cells than the ⟨111⟩ component. Very remarkably, the near-⟨100⟩ cells either formed narrow bands between wider ⟨111⟩ bands, the finest ⟨100⟩ bands being only one dislocation cell wide, or they were dispersed singly or in small clusters in a matrix comprising other orientations, *e.g.*, ⟨013⟩ and ⟨123⟩, but both morphologies constituted parts of intricate patterns. Still, for neither component were the orientations sharply defined but were scattered about the ideal orientation according to the average misorientation among the individual cells.

More recent studies of DBs have been performed in connection with rolling or channel die compression of fcc metals, with particular emphasis on the experimentally observed decomposition of the (100)[100] orientation. In a pioneering study, Akef and Driver[48] considered variations of Aernoudt and Stuwe's[49] earlier relaxed constraints model of combinations of complementary shears of opposite signs. By this means, they successfully analyzed and confirmed through experiment on (001)[010] and (001)[110] oriented aluminum crystals that the orientation decomposition occurs through DBs deforming with single and coplanar double glide, respectively. As expected, in the latter case, the bands were arranged with alternating sense of rotation. This work also includes very interesting optical slip band micrographs, some of which are remarkably similar to micrographs by Pfeil. In particular, Figures 5(b) and (c) by Akef and Driver[48] (our Figures 6(a) and 6(b)) resemble Figures 10 and 12 by Pfeil,[39] demonstrating that the patterns arise through slip system avoidance largely independent of the specific crystallography of the systems and thus specific Burgers vectors involved. Maurice and Driver[50] further concluded for Al and Al-1 pct Mn that above 300 °C ($0.6T_M$) the cube orientation was stable and DBs ceased to form in cube-oriented crystals. Above 300 °C, these crystals instead deformed in stable cube orientation "by double slip on {110}⟨1-10⟩ systems," a claim which presumably will stimulate efforts of verification by others. By contrast, "(001)[110] crystals decompose(d) at all temperatures into deformation bands of complementary {112}⟨11-1⟩ orientations."[50]

Other varied observations on DBs in connection with compression or rolling of large oriented crystals have been reported by Tsuji *et al.*[51] on cold-rolled austenitic stainless steel with columnar crystals (Part I) and the resulting recrystallization structure (Part II); they were reported by Wrobel *et al.*[52] for rolled copper crystals in cube and other orientations. Last, but not least, Lee and co-workers[53–59] published a series of articles on rolled copper of two different grain sizes as well as α brass,[56] also grounded on the model by Aernoudt and Stuwe.[49] For the case of copper, they could trace the four major rolling texture components to narrow DBs parallel to the rolling plane and stacked in an irregular order, in fact including almost certainly secondary banding in primary bands. They further achieved a significant improvement in the rolling texture model by assuming the operation of only two slip systems per band.

D. *Studies on Underlying Dislocation Microstructures and Lattice Reorientations*

The evidence presented previously strongly suggests, if not proves, that all DBs are associated with multiple texture

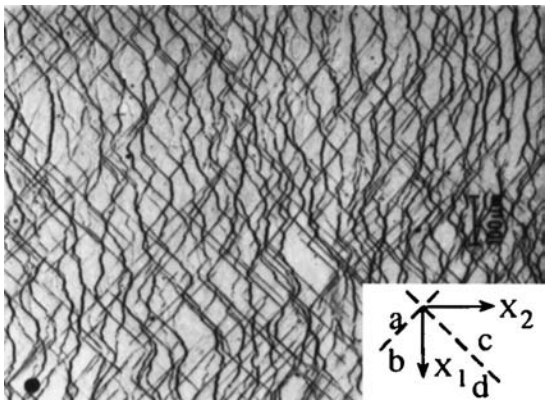

(*a*)

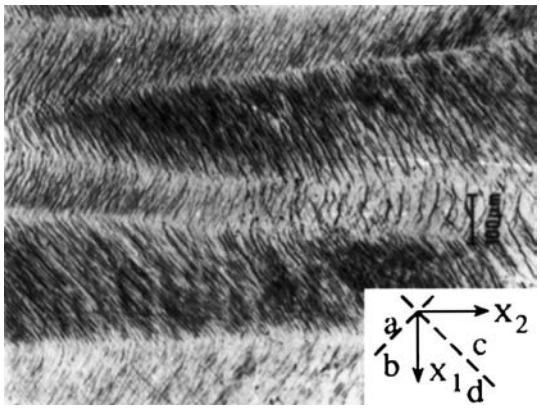

(*b*)

Fig. 6—Optical micrographs of slip bands on (001)[110] oriented aluminum crystals: (*a*) compression face at $\varepsilon = 0.15$ with no indication of DBs; and (*b*) at $\varepsilon = 0.5$ revealing DBs (Figs. 5(b) and (c) from Akef and Driver[48]).

components. But, are conversely all multiple texture components associated with DBs? From the simultaneous cessation of deformation banding and texture splitting at 300 °C in Maurice and Driver's[50] cube-oriented compressed crystals, one might incorrectly conclude that this is so. However, the discussed occasional distribution of ⟨100⟩ cells or equiaxed ⟨100⟩ cell clusters within ⟨111⟩ surroundings in Reed and McHargues[47] samples proves otherwise. As an apparently intermediate case between these two extremes, in a study of channel-die compressed pure aluminum single crystals deformed at between 473 to 773 K (0.5 and $0.8T_M$), Theyssier *et al.*[60] observed slablike "cell blocks" of varying thickness with complementary alternating lattice rotations but did not report DBs.

Sooner or later the causes for one or the other behavior will presumably be discovered through investigations on the evolution of dislocation microstructures independent of DBs. In the line of succession of References 17 through 19, specifically Cizek *et al.*[61,62] have conducted some excellent relevant work on the development of angular misorientations within grains. From their study of the development of dislocation boundaries in two individual grains of aluminum extended at 150 °C,[61] they concluded that higher-angle boundaries develop gradually from cell walls but without evidence which, if any, were true GNBs. In their follow-up article using highly ⟨100⟩ textured aluminum at 250 °C,[62] again boundaries are classed into IBs and GNBs with angular

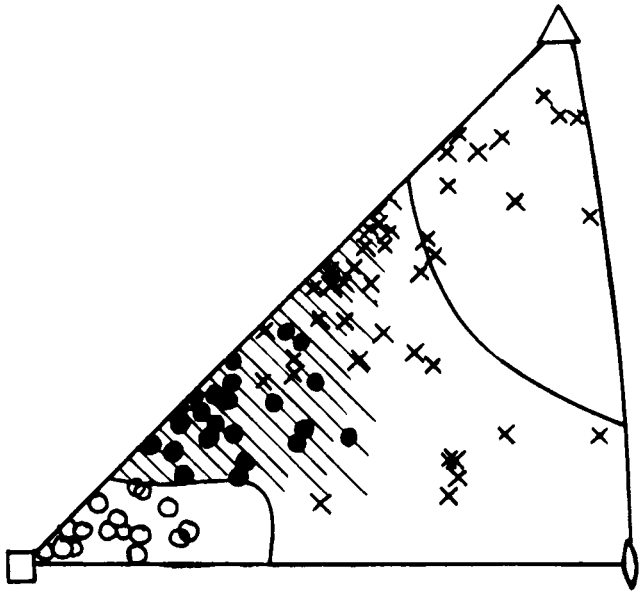

Fig. 7—Axis orientations of individual crystals in polycrystalline aluminum tensile specimens with dislocation cell structures of type 1 (○), type 2 (●), and type 3 (×) according to Hansen and Huang,[69,70,71] in relation to the domains near [100] and [111] within which Ahlborn[34] observed the axes of drawn fcc single crystals to rotate toward ⟨100⟩ and ⟨111⟩, respectively. For explanation of shading see text.

misorientation below 0.3 deg and averaging about 5 deg ranging up to 23 deg, respectively, but lacking evidence to what extent the latter might have been near an expected texture component and/or surrounded by true GNBs. In any event, the morphology was not bandlike.

In the same line, a wealth of detailed observations awaiting further analysis and classification has been accumulated by Hansen and co-workers,[63–71] almost all on cold-rolled or compressed aluminum. In these articles, various connections between microstructures, dislocation movements, mechanical properties, deformation banding, and needed adjustments in texture modeling have been established, but no cohesive picture has as yet emerged. Apparently un-noticed by the authors, their observations strongly support the "LEDS principle" and the "LEDS hypothesis," the main tenets of the LEDS theory[22,25,72–74] to be discussed in Part II.

The indicated gap in cohesive interpretation is illuminated by perhaps the most exciting part of the series, due to Hansen and Huang.[69,70,71] They derived the tensile stress-strain curve and its dependence on orientation from the dislocation structure. Herein the point of potentially great importance is the classification of dislocation cell structures into three distinctive types, dubbed types 1, 2, and 3, and their dependence on individual grain orientations relative to the tensile axis in a polycrystalline sample (Figure 7). Comparison with Figure 13 of Reference 42 suggests that the three-microstructure types are correlated with Ahlborn's three fields in the stereographic triangle, also shown in Figure 7, one of them subdivided as indicated by shading. Ahlborn's results pertain to wire-drawn (and by implication tensile-tested) fcc crystals. The three fields in the standard triangle of Figure 7 represent the following. (1) The region near the ⟨100⟩ ⇒ axis rotates toward ⟨100⟩. This behavior appears to be correlated with Hansen and Huang's type 2 microstructure that is composed of roundish cells reminiscent of the ⟨100⟩

component in Reed and McHargue's work.[47] (2) Region near the ⟨111⟩ ⇒ axis rotates toward ⟨111⟩. The correlated microstructure appears to be Hansen and Huang's type 3 composed of smaller, less-well-defined cells that are elongated parallel to the most highly stressed 45 deg plane. (3) The remainder of the triangle with, in Figure 7, a shaded part extending from the ⟨100⟩/⟨111⟩ line toward the center ⇒ initial orientations, which split into ⟨100⟩ and ⟨111⟩ components, and in the shaded region, but not outside of it, have already so split. The latter area is believed to be correlated with Hansen and Huang's bandlike type 1 microstructure, apparently delineated by the most highly stressed {111} plane, while before splitting, type 3 prevails.

If verified by further observations, these correlations would constitute a decisive advance in linking microstructures to lattice reorientations. Albeit, rather incongruously, the authors[71] make the connection between their three types of dislocation structure and lattice orientation *via* Figure 3, *i.e.*, *via* homologous deformation through the simultaneous operation of at least five equally stressed slip systems. Similarly, in their theoretical analysis of the stress-strain curve, they use the *M* factors of Figure 3. However, the probable correlation proposed by means of Figure 7 strongly suggests that at any one time only one or two systems acted together locally. Hence, the *M* factors of Figure 1 or those of the two most highly stressed systems in Figure 2 would have been appropriate. Correspondingly, the *M* values in Reference 71, and thereby the inferred tensile stresses, are presumably overestimated by factors of up to 1.5. However, since good agreement between the experimental and theoretical data was found,[71] this discrepancy of Taylor factors was presumably compensated by some other error(s).

Of some lesser interest for the present article is a recent study by Zolotorevski *et al*.[75] By means of a novel X-ray method, these authors studied orientation changes within large grains of aluminum extended up to 15 pct. They observed nonuniform, small (up to 4 deg), and mostly unexpected orientation changes. Partly, these suggest the development of DBs. However, the resolution of the technique is limited by the X-ray beam diameter of a few tenths of a millimeter, and no correlated TEM micrographs were obtained. Moreover, the results are probably atypical for general polycrystalline deformation, since the grains were pancake shaped in a 1-mm thick sample, significantly smaller than the grain diameters in the plane of the sample.

Last, of fundamental relevance are the following: (a) the conclusion by Fjeldly and Roven[76] that the relaxed constraints model (*i.e.*, by implication DBs) describes the textures of extruded Al-Zn-Mg alloy better than the Taylor model; and (b) the fact that Vandermeer and Juul Jensen[77] have been able to arrive at a quantitative interpretation of the recrystallization and growth kinetics of rolled copper by including preferential nucleation at grain and deformation band boundaries.

E. *Transition Bands*

Just as it is not necessary that segregation of complementary slip system selections assume the morphology of parallel slabs, thereby forming DBs, so also it is not necessary that the boundaries between the complementary volume elements of a deformation band structure be sharp. Rather, instead of an abrupt change of angular orientation, accommodated by the corresponding large-angle "geometrically necessary boundaries," it is possible that the boundaries between adjacent DBs be formed of layers of dislocation cells of gradual changing orientation, so as to accommodate the same angular misorientation over some width. Such slablike regions between DBs are called "transition bands" (TBs).

The first example ever of TBs seems to have been observed by Grzemba and Hu[78] in rolled cube-oriented iron crystals. The selection of Burgers vectors and arrangement of walls involved therein were later shown to be in harmony with the LEDS theory.[79] The great majority of observations made on DBs in the literature give no evidence for transition bands. However, an outstandingly fine example, not just of isolated, restricted TBs but of a continuum, was documented by Lee *et al.*,[55,58] namely, in the form of a nearly sinusoidal orientation variation in the *B* texture component parallel to the rolling plane of copper.

II. OUR OBSERVATIONS OF DEFORMATION BANDS

A. *Experimental Conditions*

Judging from the brief literature survey in the previous section, the majority of researchers in the areas of plastic deformation and dislocation structures are only peripherally aware of DBs, or at the least do not adequately connect evidence regarding DBs to their own research. Except for researchers in the area of deformation texture modeling, the prevailing opinion appears to be that DBs are a curiosity that for most purposes may be safely disregarded. In fact, it seems that DBs have never been studied for their own sake, but rather because they were observed more or less accidentally or in the course of deformation texture studies. Yet, as will be further discussed in Part II, DBs are of intense intrinsic interest, and they have far-reaching implications for plastic deformation in general and prospect for successful constitutive equations in particular.

Our own interest in DBs stems from their incidental observation in a study of the recrystallization behavior of two high-purity, low-concentration aluminum alloys.[81] Al-0.5 wt pct Cu and Al-0.5 wt pct Cu-1.0 wt pct Si, supplied by Materials Research Corporation in the form of direct chill-cast cylindrical billets (130 mm diameter and 110 mm high). They were received in the as-cast condition and homogenized in a circulating air furnace at 500 °C for 6 hours. Samples of 1.0 cm diameter and 1.5 cm height were compressed to between 50 and 80 pct + reduction of height between lubricated parallel anvils, at ambient temperature, −196 °C (liquid nitrogen), and 200 °C, in a range of strain rates. For metallographic examination, the samples were cut across the midplane parallel to the anvils, polished with diamond paste followed by a colloidal silica solution on microcloth, and then anodized at an applied voltage of 20 V for 30 seconds in a solution of 40 mL HBF_4 in 760 mL distilled water. The resulting etch is invisible under ordinary illumination but reveals grains and deformation bands when viewed between crossed polarizer/analyzer pairs.

Several micrographs of the observed deformation band structures have been presented in previous articles.[20,81] Figures 8 through 11 give additional examples among an unfortunately too restricted selection. This happened because the

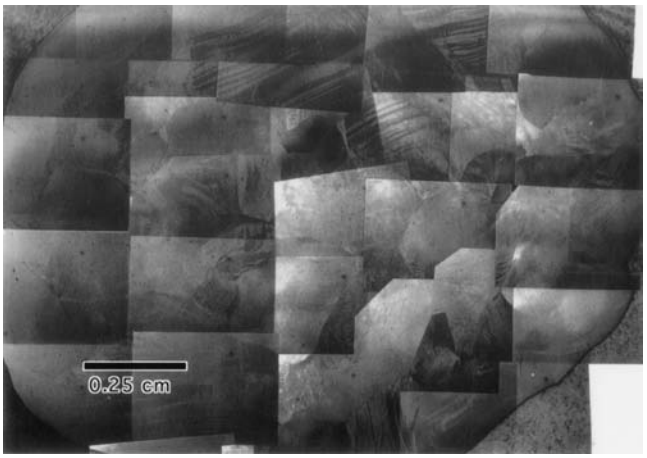

Fig. 8—Optical micrograph of the mid–cross section of a cylindrical high-purity Al-0.5 pct Cu specimen compressed at −196 °C to −0.47 true strain, etched to reveal lattice misorientations. The specimen had a moderate ⟨100⟩ texture.

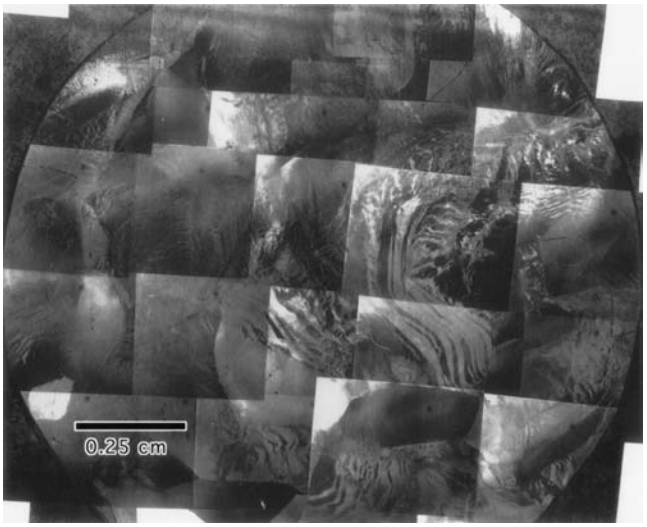

Fig. 9—Optical micrograph of the mid–cross section of a cylindrical high-purity Al-0.5 pct Cu specimen compressed at −196 °C to −0.68 true strain, etched to reveal lattice misorientations.

underlying thesis research[80] was focused on recrystallization and was completed with only a few samples remaining in the as-deformed condition when the great intrinsic interest of the deformation banding was realized. The examples in Figures 8 through 12 are montages showing the structure over most of the respective specimens, compressed at temperatures between −196 °C and 200 °C to strains between 50 pct and 80 pct height reduction, as indicated. The correlated stress-strain curves are shown in Figures 13 and 14. The gradations of overall gray shadings indicate the different lattice orientations. X-ray analysis revealed a moderate ⟨100⟩ texture in all samples, and thus the darkness variations among the grains are not as large as they otherwise would be. Also, the evolution of DBs is favored by a ⟨100⟩ texture, as first observed by Barrett and Levenson.[29]

B. *The Effect of Precipitates on CBs*

The immediately most obvious feature of the micrographs is the smaller grain size and very much weaker development

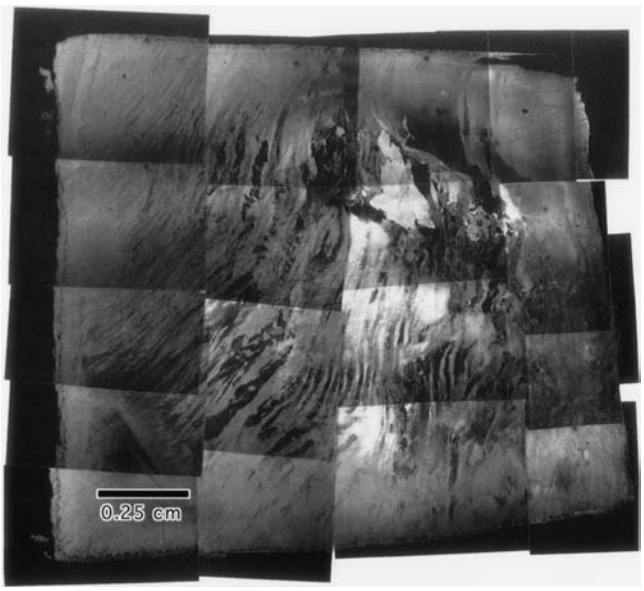

Fig. 10—Optical micrograph of the mid–cross section of a cylindrical high-purity Al-0.5 pct Cu specimen compressed at room temperature to −0.72 true strain, etched to reveal lattice misorientations.

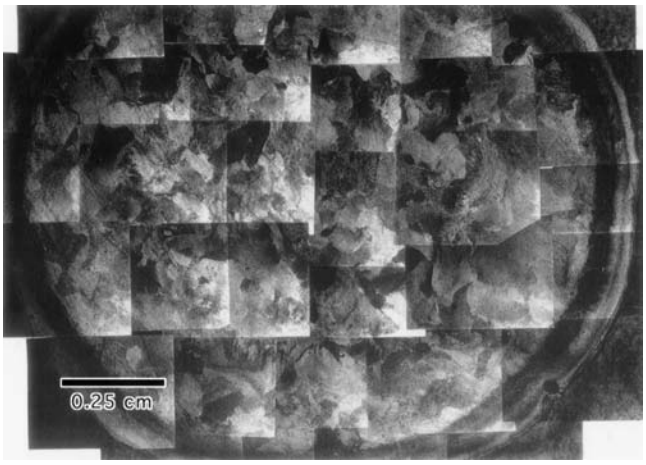

Fig. 11—Optical micrograph of the mid–cross section of a cylindrical Al-Cu-Si alloy deformed to −0.69 true strain at room temperature, etched to reveal lattice misorientations. Only a minority of the grains exhibits deformation bands.

of deformation banding in the inhomogeneous (Figures 11 and 12) as compared to the homogeneous alloy (Figures 8 through 10). Both of these features are doubtlessly due to the presence of the precipitates, as follows. (a) The grain refining effect of precipitates is, of course, well known. (b) Seeing that DBs form in response to relatively minor stress differences among slip system selections, the effect of precipitates to inhibit DBs is intuitively expected, namely, through their surrounding random internal stresses.

C. *DB Morphology as a Function of Strain and Grain Size*

The most obvious differences in appearance between Figures 8 and 9 as compared to Figure 10 are due to the fact that the edges of the sample in Figure 10 were trimmed to

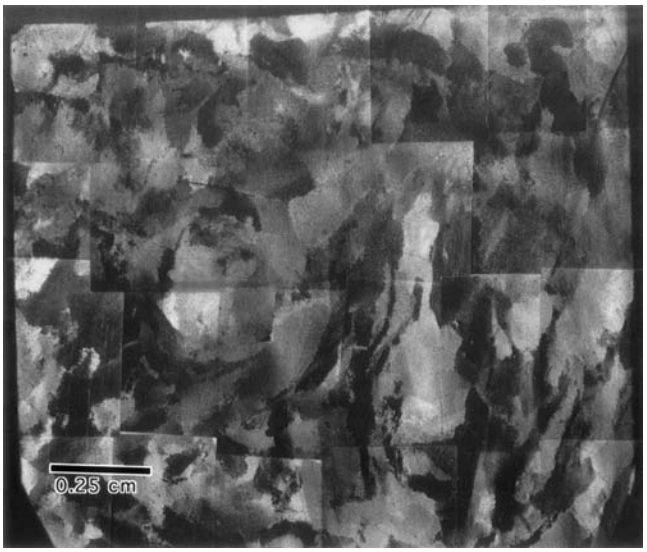

Fig. 12—Optical micrograph of the mid–cross section of a cylindrical Al-Cu-Si alloy deformed to −0.69 true strain at 200 °C, etched to reveal lattice misorientations. Almost no DBs can be found.

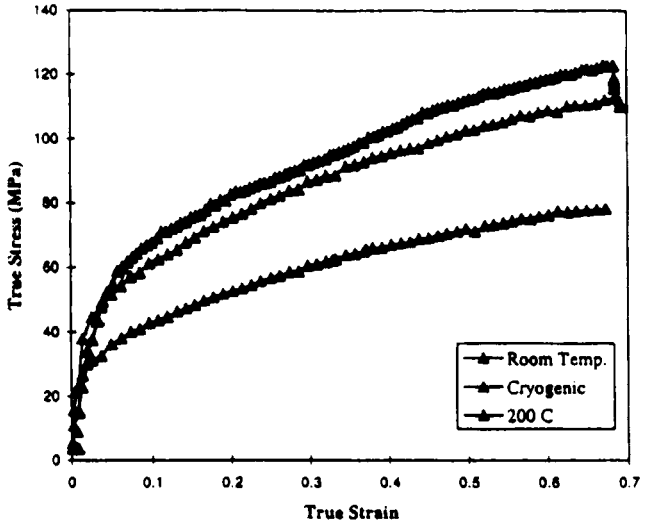

Fig. 13—True stress–true strain compression curves for the Al-0.5 pct Cu alloy at 1 pct per second strain rate at −196 °C (cryogenic), room temperature, and 200 °C as indicated.

accommodate the restricted size of the X-ray diffractometer; the same trimming was similarly done on the sample in Figure 12. The resulting damage seemingly affected the etching about the periphery in Figure 10, but also in the other samples, the etching tends to deteriorate toward the edges.

Comparison between Figures 8 and 9, both of which pertain to compression at cryogenic temperature but differ in the amount of strain, shows through the increasing contrast differences that the average angular misorientation among the bands increases with strain. This is expected as the orientations within DBs approach those of the fully developed texture components, beginning from a unitary orientation (compare the orientation fields in Figure 7 due to Ahlborn). Comparison between Figures 8 and 9 also indicates that the DBs are initially bounded by low-index crystallographic planes and through further compression become

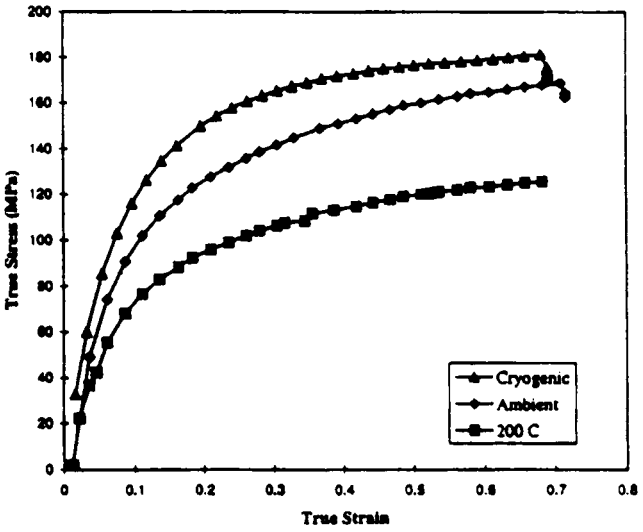

Fig. 14—True stress–true strain compression curves for the Al-0.5 pct Cu-1 pct Si alloy at 1 pct per second strain rate at −196 °C (cryogenic), room temperature, and 200 °C as indicated.

distorted as they deform along with the material as a whole. Since the DBs are delineated by dislocation rotation boundaries of somewhat restricted mobility, such global distortions are not surprising. They are thus an indicator of the deviation of actual polycrystalline strain from the unitary grain deformation assumed alike in the Sachs/Boas and Schmid/Taylor/Bishop and Hill models; this is quite apart from the complementary alternating strains in the DBs. Indications from Figures 8 and 9 are that this global bending and twisting of the individual grains in our samples of carefully uniaxially compressed fcc metal is moderate up to about 50 pct strain but becomes fairly severe at larger strains.

The micrographs show that DBs do not cross grain boundaries, although they can be continued by similar DBs on the other side. By contrast, families of DBs profusely cross each other, and higher magnifications (*e.g.*, Reference 81) reveal plentiful secondary within primary bands. As seen in the micrographs and will be further explained in Part II, band lengths and widths are correlated to the effect that longer bands are also wider so that smaller grains exhibit a finer banding. Moreover, larger grains are evidently more prone to develop DBs than smaller ones, so that small grains tend to have weaker or no DBs.

Perhaps the most impressive feature of Figures 8 through 10 is the sheer size of the largest DBs, that is limited only by the size of the grains. Thus, the DBs range up to 0.5-cm long and a 3-mm wide; in fact, they are easily visible with the naked eye. Barrett and Levenson[28] observed even longer DBs in aluminum, namely, about 4-cm long and 1-mm wide extending inward from a surface and 1-cm long and 0.6-mm wide in an interior grain. This may be compared with the average dislocation cell size of about 0.5 μm in our case and perhaps 1 μm in Reference 28. Hence, the largest DBs utterly dwarf the dislocation cells. Yet, the smallest secondary and tertiary bands may be only a few dislocation cell sizes across.[47,81]

D. *Effect of Deformation Temperature*

In line with the evidence that DBs cease to form as the deformation temperature is raised (*e.g.*, Reference 50), the

Al-Cu-Si alloy exhibits only minor deformation banding after compression at ambient temperature (Figure 11) and virtually none at 200 °C (Figure 12). Similarly, in the Al-Cu alloy, DBs are very weak or absent at 200 °C and above. Perhaps very important in this connection is the apparent rise of orientation nonuniformity within individual bands with increasing deformation temperature suggested by Figures 8 and 9 in comparison with Figure 10. Specifically, in Figure 10, pertaining to room temperature compression, note the variable shading within DBs, as compared to the much greater uniformity after deformation at −196 °C seen in Figures 8 and 9.

At this point, it seems very likely that this deterioration of lattice orientation uniformity within bands is part and parcel of the temperature dependence of deformation band formation. Namely, with rising deformation temperatures, progressive orientation variability will sooner or later obliterate the bands entirely. Such statistical misorientations within DBs are closely comparable to the local orientation differences about precipitates. Correspondingly, it is tentatively proposed that DB reduction through precipitates and through rising deformation temperatures are explained by basically the same phenomenon. However, much more evidence will be required before these conclusions can be safely drawn.

III. INTEGRATION WITH THE THEORY OF CRYSTAL PLASTICITY

As greatly important as CBs evidently are based on the evidence already presented, perhaps their greatest significance lies in their impact on recrystallization. This is so because deformation band boundaries are preferred sites for grain nucleation, as first demonstrated by Pfeil[39] for the case of compressed iron crystals. Additionally, they impact recrystallization as DB boundaries may move so as to expand one of the components at the expense of the other(s). Thus, Vandermeer and McHargue[82] observed the ⟨100⟩ component in the double fiber texture to grow at the expense of the ⟨111⟩ component through migration of the DB boundaries.

In view of the discussed role of DBs in recrystallization, we have already pointed to the recent analysis by Vandermeer and Juul Jensen,[77] which demonstrated the importance of preferred grain nucleation at two-dimensional surfaces. Of course, grain boundaries are the most obvious candidates to play that role. However, if deformation banding occurs, the total area of DB boundaries, including secondary and tertiary band boundaries, absolutely swamps that of the grain boundaries. Considering, then, the peculiar and otherwise unexpected orientation relationships which develop at DB boundaries, among primary, secondary, and even tertiary bands, what are our chances of arriving at a predictive theory of recrystallization unless deformation banding is quantitatively understood?

Finally, and perhaps most importantly, the phenomenon of deformation banding is a potentially most valuable tool for the understanding of the mechanism of plastic deformation, without which there is no realistic prospect for the construction of technologically useful constitutive equations. This aspect will be discussed in Part II.

ACKNOWLEDGMENTS

Thanks are due to M.S. Bednar for doing some of the metallographic work beyond the call of duty. One of the authors (SSK) acknowledges the support of the Materials Research Corporation. The financial support of the National Science Foundation under grant No. DMR-9814768, Dr. Bruce MacDonald, Program Manager is gratefully acknowledged.

REFERENCES

1. E. Schmid and W. Boas: *Plasticity of Crystals*, Chapman and Hall, Ltd., London, 1950 (translated from original 1935 German edition).
2. G. Sachs: *Z. Ver. Deutsch. Ing.*, 1928, vol. 72, pp. 734-36.
3. W. Boas and E. Schmid: *Z. Technol. Phys.*, 1931, vol. 12, pp. 71-75.
4. R. von Mises: *Z. Angew. Math. Mech.*, 1928, vol. 8, pp. 161-85.
5. G.I. Taylor: *J. Inst. Met. (London)*, 1938, vol. 62, pp. 307-24; *S. Timoshenko Anniversary Volume*, MacMillan and Co, New York, NY, 1938, pp. 218-24.
6. J.F.W. Bishop and R. Hill: *Phil. Mag.*, 1951, vol. 42, pp. 414-27 and 1298-1307.
7. G.Y. Chin and W.L. Mammel: *Trans. TMS-AIME*, 1969, vol. 245, pp. 1211-14.
8. G.Y. Chin and W.L. Mammel: *Trans. TMS-AIME*, 1967, vol. 239, pp. 1400-05.
9. C.F. Elam: *Proc. R. Soc.*, 1927, vol. 115, p. 148.
10. M. Masima and G. Sachs: *Z. Phys.*, 1928, vol. 50, p. 161.
11. H. Wilsdorf and D. Kuhlmann-Wilsdorf: *Z. Angew. Phys.*, 1952, vol. 4, pp. 361-70.
12. P.J. Jackson and Z.S. Basinski: *Can. J. Phys.*, 1967, vol. 45, pp. 707-33.
13. H.-W. Wu, M.A. Przystupa, and A.J. Ardell: *Metall. Mater. Trans. A*, 1997, vol. A28, pp. 2353-60.
14. R. Becker: *Acta Metall. Mater.*, 1991, vol. 39, pp. 1211-30.
15. G.B. Sarma and P.R. Dawson: *Acta Mater.*, 1996, vol. 44, pp. 1937-53.
16. P.R. Dawson and A.J. Beaudoin: in *Texture and Anisotropy*, U.F. Kocks, C.N. Tome, and H.-R. Wenk, eds., Cambridge University Press, Cambridge, United Kingdom, 1998, pp. 512-31.
17. B. Bay, N. Hansen, and D. Kuhlmann-Wilsdorf: *Mater. Sci. Eng.*, 1989, vol. A113, pp. 385-97.
18. B. Bay, N. Hansen, and D. Kuhlmann-Wilsdorf: *Mater. Sci. Eng.*, 1992, vol. A158, pp. 139-46.
19. B. Bay, N. Hansen, D.A. Hughes, and D. Kuhlmann-Wilsdorf: *Acta Metall. Mater.*, 1992, vol. 40, pp. 205-19.
20. D. Kuhlmann-Wilsdorf: *Acta Mater.*, 1999, vol. 47, pp. 1697-1712.
21. D. Kuhlmann-Wilsdorf and N. Hansen: *Scripta Metall. Mater.*, 1991, vol. 25, pp. 1557-62.
22. D. Kuhlmann-Wilsdorf: *Phys. Status Solidi*, 1995, vol. (a) 149, pp. 225-41.
23. D. Kuhlmann-Wilsdorf: *Scripta Metall. Mater.*, 1996, vol. 34, pp. 641-50.
24. D. Kuhlmann-Wilsdorf: *Scripta Metall. Mater.*, 1997, vol. 36, pp. 173-81.
25. D. Kuhlmann-Wilsdorf: *Mater. Res. Innov.*, 1998, vol. 1, pp. 265-97.
26. D. Duly, G.J. Baxter, H.R. Shercliff, J.A. Whiteman, C.M. Sellars, and M.F. Ashby: *Acta Mater.*, 1996, vol. 44, pp. 2947-62.
27. C.S. Barrett: *Trans. AIME*, 1939, vol. 135, pp. 296-324.
28. C.S. Barrett and H. Levenson: *Trans. AIME*, 1939, vol. 135, pp. 327-43.
29. C.S. Barrett and H. Levenson, *Trans. AIME*, 1940, vol. 137, pp. 112-26.
30. C.S. Barrett and F.W. Steadman: *Trans. AIME*, 1942, vol. 147, pp. 57-66.
31. C.S. Barrett: *Structure of Metals: Crystallographic Methods, Principles and Data*, McGraw-Hill, New York, NY, 1943, pp. 381-419.
32. C.S. Barrett and T.B. Massalski: *Structure of Metals*, 3rd ed., McGraw-Hill, New York, NY, 1966.
33. J. Hirsch and K. Lucke: *Acta Metall.*, 1988, vol. 36, pp. 2863-82 and 2883-2904.
34. J. Hirsch, K. Lucke, and M. Hatherly: *Acta Metall.*, 1988, vol. 36, pp. 2905-27.
35. *8th Int. Conf. on Textures of Materials*, J.M. Kallend and G. Gollstein, eds., TMS, Warrendale, PA, 1988.
36. *Textures of Materials*, ICOTOM 11, Z. Liang, L. Zuo, and Y. Chu, eds., International Academic Publishers, Beijing, 1996.

37. *Texture and Anisotropy*, U.F. Kocks, C.N. Tome, and H-R Wenk eds., Cambridge University Press, Cambridge, United Kingdom, 1998.
38. I.B. Pfeil: Carnegie Schol. Mem., *Iron Steel Inst.*, 1926, vol. 15, pp. 319-78.
39. I.B. Pfeil: Carnegie Schol. Mem., *Iron Steel Inst.*, 1927, vol. 16, pp. 153-210.
40. G.I. Taylor and C.F. Elam: *Proc. R. Soc. (London)*, 1927, vol. 112, pp. 337-61.
41. H. Ahlborn: *Z. Metallkd.*, 1965, vol. 56, pp. 205-15.
42. H. Ahlborn: *Z. Metallkd.*, 1965, vol. 56, pp. 411-20.
43. H. Ahlborn: *Z. Metallkd.*, 1966, vol. 57, pp. 887-84.
44. H. Ahlborn: *Recrystallization, Grain Growth and Textures*, ASM, Metals Park, OH, 1966, pp. 374-81.
45. G.Y. Chin and B.C. Wonsiewicz: *Trans. AIME*, 1969, vol. 245, pp. 871-72.
46. G.Y. Chin: *Textures in Research and Practice*, Springer, Berlin, 1969, pp. 51-80.
47. R.E. Reed and C.J. McHargue: *Trans. AIME*, 1967, vol. 239, pp. 1604-12.
48. A. Akef and J.H. Driver: *Mater. Sci. Eng.*, 1991, vol. A132, pp. 245-55.
49. E. Aernoudt and H.P. Stuwe: *Z. Metall.*, 1970, vol. 61, pp. 128-36.
50. C. Maurice and J.H. Driver: *Acta Metall. Mater.*, 1993, vol, 41, pp. 1653-64.
51. N. Tsuji, H. Takebayashi, T. Takiguchi, K. Tsuzaki, and T. Maki: *Acta. Metall. Mater.*, 1955, vol. 43, pp. 743-54 and 755-68.
52. M. Wrobel, S. Dymek, M. Blicharski, and S. Gorczyca: *Z. Metallkd.*, 1994, vol. 85, pp. 415-425.
53. B.J. Duggan and C.S. Lee: *Scripta Metall. Mater.*, 1992, vol. 27, pp. 1503-07.
54. C.S. Lee, B.J. Duggan, and R.E. Smallman: *Acta Metall. Mater.*, 1993, vol. 41, pp. 2265-70.
55. C.S. Lee and B.J. Duggan: *Acta Metall. Mater.*, 1993, vol. 41, pp. 2691-99.
56. C.S. Lee and B.J. Duggan: *Mater. Sci. Technol.*, 1994, vol. 10, pp. 155-61.
57. C.S. Lee, R.E. Smallman, and B.J. Duggan: *Mater. Sci. Technol.*, 1994, vol. 10, pp. 862-68.
58. R.E. Smallman and C.S. Lee: *Mater. Sci. Eng.*, 1994, vol. A184, pp. 97-112.
59. C.S. Lee, R.E. Smallman, and B.J. Duggan: *Scripta Metall. Mater.*, 1995, vol. 33, pp. 727-33.
60. M.C. Theyssier, B. Chenal, J.H. Driver, and N. Hansen: *Phys. Status Solidi*, 1995, vol. (a)149, pp. 367-78.
61. P. Cizek, B.A. Parker, and B.J. Wynne: *Scripta Metall. Mater.*, 1995, vol. 32, pp. 319-23.
62. P. Cizek, B.A. Parker, and B.J. Wynne: *Scripta Mater.*, 1996, vol. 35, pp. 1129-34.
63. D.A. Hughes, Q. Liu, D.C. Chrzan, and N. Hansen: *Acta Mater.*, 1997, vol. 45, pp. 105-12.
64. G. Winther, D. Juul Jensen, and N. Hansen: *Acta Mater.*, 1997, vol. 45, pp. 2455-65.
65. J.A. Wert, Q. Liu, and N. Hansen: *Acta Mater.*, 1997, vol. 45, pp. 2565-76.
66. D.A. Hughes and N. Hansen: *Acta Mater.*, 1997, vol. 5, pp. 871-86.
67. G. Winther, D. Juul Jensen, and N. Hansen: *Acta Mater.*, 1997, vol. 45, pp. 5059-68.
68. A. Godfrey, D. Juul Jensen, and N. Hansen: *Acta Mater.*, 1998, vol. 46, pp. 823-33 and 835-48.
69. X. Huang and N. Hansen: *Scripta Metall.*, 1997, vol. 37, pp. 1-7.
70. N. Hansen and X. Huang: *Mater. Sci. Eng.*, 1997, vols. A234–A236, pp. 602-05.
71. N. Hansen and X. Huang: *Acta Mater.*, 1998, vol. 46, pp. 1827-36.
72. D. Kuhlmann-Wilsdorf: in *Workhardening*, J.P. Hirth and J. Weertman, eds., Gordon and Breach, New York, NY, 1968, pp. 97-132.
73. D. Kuhlmann-Wilsdorf: *Mater. Sci. Eng.*, 1989, vol. A113, pp. 1-41.
74. D. Kuhlmann-Wilsdorf: *Phil. Mag.*, 1999, vol. 79, pp. 955-1008.
75. N.Y. Zolotorevski, Y.F. Titovets, and G.Y. Dyatlova: *Scripta Mater.*, 1998, vol. 38, pp. 1263-68.
76. A. Fjeldly and H.J. Roven: *Acta Mater.*, 1996, vol. 44, pp. 3497-3504.
77. R.A. Vandermeer and D. Juul Jensen: *Metall. Mater. Trans. A*, 1995, vol. 26A, pp. 2227-35.
78. B. Grzemba and H. Hu: *Z. Metallkd.*, 1969, vol. 60, pp. 944-48.
79. D. Kuhlmann-Wilsdorf and E. Aernoudt: *J. Appl. Phys.*, 1983, vol. 54, pp. 184-92.
80. S.S. Kulkarni: Master's Thesis, University of Virginia, Charlottesville, VA, 1997.
81. S.S. Kulkarni, E.A. Starke, Jr, and D. Kuhlmann-Wilsdorf: *Acta Metall. Mater.*, 1998, vol. 46, pp. 5283-5302.
82 R.A. Vandermeer and C.J. McHargue: *Trans. AIME*, 1964, vol. 230, pp. 667-75.